Link-based performance optimization of spatial mechanisms

Yimesker Yihun
Dep. of Mechanical Engineering
Idaho State University
Pocatello, Idaho, USA

Email: yimeyihu@isu.edu

Ken Bosworth
Dep. of Mechanical Engineering
and Dep. of Mathematics
Idaho State University
Pocatello, Idaho, USA
Email: boswkenn@isu.edu

Alba Perez-Gracia
Dep. of Mechanical Engineering
Idaho State University
Pocatello, Idaho, USA
Email: perealba@isu.edu

In the design of spatial linkages, the finite-position kinematics is fully specified by the position of the joint axes, i.e., a set of lines in space. However, most of the tasks have additional requirements regarding motion smoothness, obstacle avoidance, force transmission, or physical dimensions, to name a few. Many of these additional performance requirements are fully or partially independent of the kinematic task and can be fulfilled using a link-based optimization after the set of joint axes has been defined.

This work presents a methodology to optimize the links of spatial mechanisms that have been synthesized for a kinematic task, so that additional requirements can be satisfied. It is based on considering the links as anchored to sliding points on the set of joint axes, and making the additional requirements a function of the location of the link relative to the two joints that it connects. The optimization of this function is performed using a hybrid algorithm, including a genetic algorithm (GA) and a gradient-based minimization solver.

The combination of the kinematic synthesis together with the link optimization developed here allows the designer to interactively monitor, control and adjust objectives and constraints, to yield practical solutions to realistic spatial mechanism design problems.

1 Introduction

The finite-position kinematic synthesis methods yield a linkage able to reach a set of specified positions. In the case of planar linkages, the links are usually located in parallel planes perpendicular to the joints, which defines their geometry to a great extent. In the case of spatial mechanisms with general relative position between joints, such as those obtained from spatial kinematic synthesis, the geometry and properties of the links can be greatly modified by just sliding the joint location along the joint axis. Notice that this operation does not modify the trajectory of the linkage.

The actual geometry and location of the links have important consequences for the performance of the linkage, including but not limited to linkage size and occupied space, self-intersections and obstacle avoidance, friction at the joints and other force transmission issues.

Most of the current and past literature focuses on the optimization for planar mechanisms, in which the kinematic synthesis -mostly approximate synthesis- and the additional requirements are solved simultaneously. The focus in most of them is in optimizing the desired trajectory or motion generation. Some commonly used optimization methods for planar mechanism design are the least-square technique with vector geometric and functional equations [1], the least-square technique with assembly constraints [2], [3] and [4], together with the use of loop equation techniques, [5], [6], [7]. Other methods include geometric constraint programming [8], and genetic algorithms ([9], [10]). In [11], the focus is on optimizing performance requirements. Also see [12], [13] and [14].

For the optimized synthesis of spatial linkages, current research focuses on using partial dimensioning to optimize some characteristics, for instance workspace, isotropy and

dexterity [15], [16], [17] or stiffness [18]; for a summary and literature review of this approach, with its challenges and shortcomings, see [19]. The definition of the *characteristic length* has also been used for the optimization of performance parameters with disparate units, see [20]. In [21], Pareto-optimal solutions are found for the optimization of kinematic and dynamic specifications. Several indices have been defined for optimizing a spatial version of the transmission index [22] and the optimization of motion/force transmissibility using screw theory [23]. The kinematic mapping can also be used for optimization. This method, started by Ravani and Roth [24], has been used in [25], [26] to optimize dimension and type of a mechanism. Optimization of spatial mechanisms using GA has been done in [27]; the work focuses on the optimization of the link lengths to obtain a closer trajectory. In the case of parallel robots [28] the focus has been to find parameters of the manipulator, whose workspace contains the specified points. Kim and Tsai [18] present the optimization of link lengths and some link position parameters for a 3-CRR parallel manipulator in order to maximize the stiffness for a given workspace volume. In [29], kinematic optimization is applied to optimize the structure of a spatial mechanism that can be used for surgical robot.

In most of the works presented, the optimization is performed to account for additional requirements and to perform approximate synthesis simultaneously. This approach has only been applied to simplified geometries, such as symmetric or planar mechanisms; the additional requirements are mostly joint-related. No general synthesis plus link optimization method exists to our knowledge, possibly due to the very high complexity of the resulting system of equations. The purpose of this work is to show that an optimization method for general spatial mechanisms to treat the synthesis and additional requirements independently is a good solution, both from the computational and from the user interaction and assessment point of view.

In our design methodology, the design process is divided into two stages. The first stage uses kinematic synthesis in order to create an articulated system able to perform a specified motion task, which consists of a set of positions in the case of finite position synthesis. This stage defines, given the type and number of joints and their connectivity, the relative position between the joints and the first joint with respect to the reference frame. This fully specifies the theoretical workspace of the mechanism, if we assume no joint limits. The second stage, which is the focus of this paper, deals with the optimization of the links to satisfy a set of performance requirements. The optimization is performed using a GA together with gradient-based minimization. The GA creates a grid of iterative points and keeps only those under a certain objective function value with respect to the previous iteration, then the output from the GA is used as an input for the gradient-based minimization to get into a global minimum point. The optimization approach is illustrated on two examples: a spatial, one-degree-of-freedom CRR-RRR closed linkage and a Bennett linkage.

The results show that the modification of the links along the joints leads to dramatic changes in the final design and performance of spatial mechanisms.

2 Link-Based Optimization

The input for the link-based optimization process is taken from the output of a previous kinematic synthesis process. The synthesis step yields a set of structural parameters that can be, depending on the synthesis methodology used, a set of points or vectors defining the axes if loop equations or geometric constraints are used [30], Denavit-Hartenberg parameters ([31], [32]) defining relative position between joint axes if forward kinematics equations are used, etc. In any case, those design parameters can be used to compute the Plücker coordinates of the joint axes at a given configuration. The selection of reference configuration is arbitrary; usually the first task position is used to define it. For instance, for an n-jointed linkage, the input data for the optimization stage is the set of joint axes

$$\{\mathsf{S}_i = \mathbf{s}_i + \varepsilon \mathbf{s}_i^0\}, \quad i = 1, \ldots n, \tag{1}$$

where $\mathbf{s}_i$ is the unit direction vector for axis S_i, $\mathbf{s}_i^0$ is the moment of the axis, obtained as the cross product of a point on the axis and the direction $\mathbf{s}_i$, and ε is the dual unit such that $\varepsilon^2 = 0$. For some methods to compute the Plücker coordinates of the joint axes from other structural data, see for instance [33].

An initial implementation of the spatial linkage can be obtained by drawing the links at the common normal lines between consecutive axes. Manual adjustment of the links can be performed by using a CAD model. The screw axes obtained from the synthesis are drawn and then the links are modified by sliding the anchor points as shown in Figure 1. This procedure can yield a mechanism which is out of a constrained region for a given configuration, or it can help reduce the length of some of the links; however, due to the high degree of nonlinearity and difficulty of visualization of spatial linkages, this process is time-consuming and does not grant an optimized solution. In this work we show that a better solution may be obtained for some of the requirements if we perform the link-sliding operation as an optimization problem.

In the following sections, the optimization algorithm is developed and tested to account for different issues that arise in spatial mechanism design, such as minimizing overall length of the linkage, avoiding interference with a given region of space, minimizing friction at the joints due to the transmission forces, or shaping a selected part/ area of

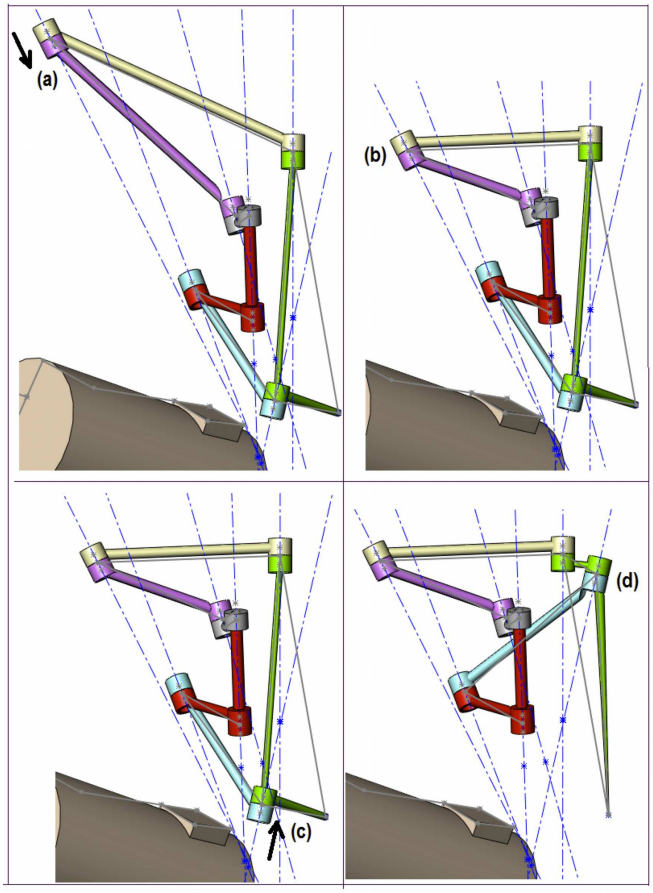

Fig. 1. CAD model for manual adjustment and optimization; Sliding anchor point from (a) to (b) and from (c) to (d)

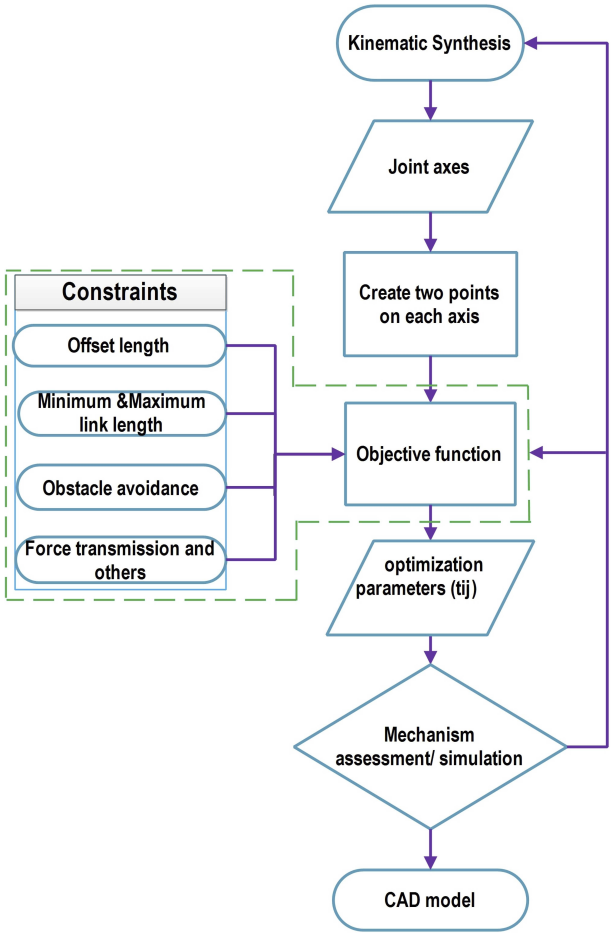

Fig. 2. Overall design strategy. Link-based optimization stages are shown inside the broken lines

a mechanism. Each of these problems can be stated -and solved- separately, or can be included in an overall optimization.

2.1 Optimization problem formulation

In the optimization, the variables to consider are the sliding parameters that define the anchoring points of the links on the joints. An objective function and additional constraints that can be written as a function of these sliding parameters. The selection of the objective function depends on the requirements of the design, and the only condition is for it to be a continuous function of the sliding parameters. Some of the possible objective functions include minimizing the overall length of the mechanism, which may help decreasing material usage, weight, inertia and overall space occupied by the mechanism; minimize friction at the joints, which helps the overall efficiency of the linkage, etc. Figure 2 shows how the optimization process fits in an overall design strategy for spatial mechanisms.

Let link ij denote the link connecting joint i to joint j. The sliding parameter t_{ij} on joint axis S_i defines the anchor point of link ij along this joint axis. Let C_i be the point on the joint axis S_i at which the line from the origin intersects the joint axis S_i at a right angle, see Figure 3. Let P_{ij} be a point on the joint axis S_i as defined in Figure 3, and t_{ij} the corresponding distance to P_{ij} from the point C_i along the direction of the axis. For a similar formulation used to detect self-intersections, see [34]. Point C_i can be obtained using

$$\mathbf{C}_i = \frac{\mathbf{s}_i \times \mathbf{s}_i^0}{\mathbf{s}_i \cdot \mathbf{s}_i}. \tag{2}$$

Then P_{ij} is expressed with respect to C_i as follows,

$$\mathbf{P}_{ij} = \mathbf{C}_i + t_{ij}\mathbf{s}_i \quad i = 1,\ldots,n. \tag{3}$$

Notice that in P_{ij}, the subscript i indicates that the point lies on joint axis S_i, while the second subscript j indicates that it also belongs to the line linking joint axis S_i with joint axis S_j. For a single-loop closed mechanism, two points need to be

defined on each axis in order to specify all links, see Figure 3 (a). For a serial robot, two points are defined in each of the axes except for the first axis. If the distance to the reference frame is a parameter of interest, the first point C_1 could be also included in the optimization as P_{10}.

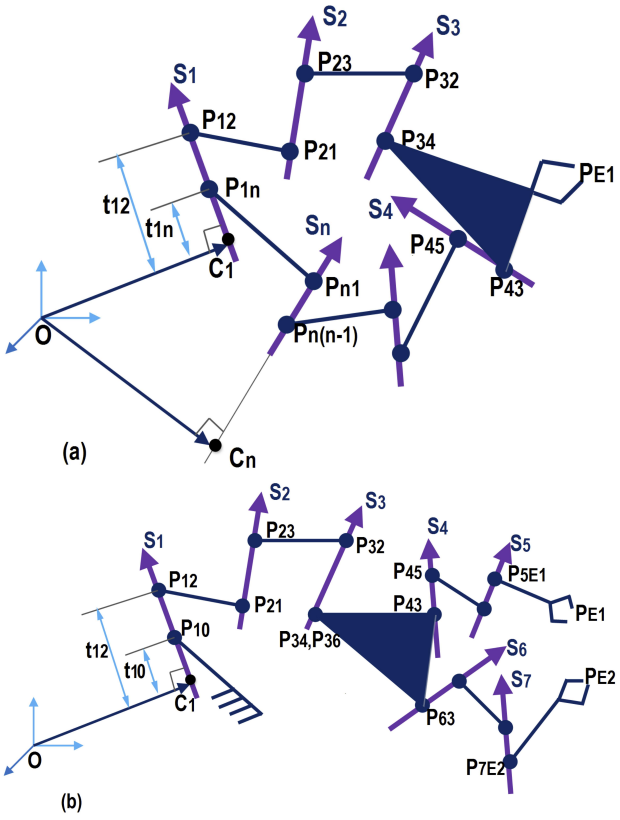

Fig. 3. Joint axes for two spatial mechanism topologies:(a) A closed linkage, CRR-RRR; (b) A linkage with a tree structure, 3R-(2R,2R)

A possible objective function is formulated to minimize the overall length by considering the offset distances along the joint axes, the lengths of the links between each pair of connected axes, as well as the length of the links to the end effectors. For example for a closed, n-jointed mechanism, the objective function is a quadratic function with $2n$ variables, the scalar slides t_{ij}. A mechanism can have multiple end effectors, like the one in Figure 3 (b); in that case, distances to each of the end effectors are also included in the objective function. For instance, equation (4) is an objective function with m number of end-effectors, where point P_{Dj} is one point in the end-effector D and point P_{Dj} is a point on axis j, and the line joining both points defines the last link on that branch. Assuming that the joints are numbered consecutively, the objective function is stated as

$$F = \Big(\sum_{i=1(\mod n)}^{n} \big((\mathbf{P}_{i,i+1} - \mathbf{P}_{i,i-1}).(\mathbf{P}_{i,i+1} - \mathbf{P}_{i,i-1}) + (\mathbf{P}_{i+1,i} - \mathbf{P}_{i,i+1}).(\mathbf{P}_{i+1,i} - \mathbf{P}_{i,i+1}) \big) + \sum_{j=1}^{m} (\mathbf{P}_{Dj} - \mathbf{P}_{jD}).(\mathbf{P}_{Dj} - \mathbf{P}_{jD}) \Big) \tag{4}$$

Using this notation, we consider S_0 to be the joint "previous to the first one". For serial chains, that defines a ground link from the reference frame, while for closed linkages, the last joint axis is the one denoted as S_0, creating a ground link between the last and first joint.

Another possible objective function can be formulated as shown in Equation (5), used to optimize the efficiency by minimizing friction for a linkage with revolute joints, imposing a certain angle of incidence of the links on the joints. Considering $\mathcal{L}$ as the set of indices ij for all links in the mechanism,

$$F = \Big(\sum_{\substack{j=1(\mod n) \\ ij \in \mathcal{L}}}^{n} \big(\frac{(\mathbf{P}_{ji} - \mathbf{P}_{ij})}{||\mathbf{P}_{ji} - \mathbf{P}_{ij}||} \cdot \mathbf{s}_j \big)^2 \Big) \tag{5}$$

Several requirements could be optimized simultaneously by using multi-objective optimization [35], [36], however in our case adding additional constraints to create a constrained optimization solves the problem efficiently. The derivation of additional constraints is shown in next section.

2.2 Additional Constraint Functions

The link-based optimization algorithm developed in this paper allows the definition of a number of linear and nonlinear constraints to satisfy link dimensions, obstacle avoidance, reduction of friction loads and manufacturability constraints. This section presents the formulation of the constraints as a function of the sliding parameters.

2.2.1 Link length and joint offset constraints

For many practical cases, constraints on the link size are required [36]. In the case of offset length, the distance between P_{ij} and P_{ik} is set to be greater than or equal to a constant value d, in order to help in the implementation of joints for ease of assembly. This adds n equality or inequality constraints,

$$\sqrt{(\mathbf{P}_{ik} - \mathbf{P}_{ij}).(\mathbf{P}_{ik} - \mathbf{P}_{ij})} \geq d, \quad i = 1, \ldots n, \tag{6}$$

which are linear in the slide parameters, yielding

$$t_{ik} - t_{ij} \geq d, \quad i = 1, \ldots n. \tag{7}$$

Similarly, a minimum and a maximum link size may be required for manufacturability and compactness. This is accomplished by setting the values l_{min} and l_{max} for the minimum and maximum link lengths respectively, which add $2n$ additional inequality constraints,

$$l_{min}^2 \leq (\mathbf{P}_{ij} - \mathbf{P}_{ji}) \cdot (\mathbf{P}_{ij} - \mathbf{P}_{ji}) \leq l_{max}^2, \quad i = 1, \ldots n, \quad ij \in \mathcal{L}. \tag{8}$$

These equations are quadratic in the link slide parameters t_{ij}.

2.2.2 Constraints for obstacle avoidance

Another common requirement is for the mechanism to avoid a certain region of space during its motion, or to establish a certain relation of closeness/separation with respect to a certain region. Here the links are modeled as cylinders, with radius R_{ij}. The obstacle region can be modeled or represented by different geometrical shapes, for instance as a cylinder with radius R_c and axis of the cylinder passing through points P_{c1} and P_{c2} as shown in the Figure 4; as a sphere with radius R_s and its center at point S_c (Figure 5); as a plane or set of planes, etc.

Within the minimization algorithm, this problem has been stated as a set of constraint functions, defined in such a way that the linkages of the mechanism must stay out of the constrained region (cylinder, sphere etc) or maintain a certain distance with respect to the region.

Cylinder constraint equations

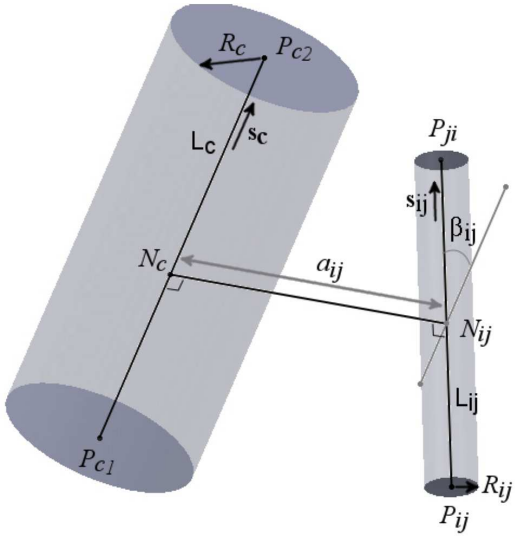

Fig. 4. Constraint Region Represented by a Cylindrical Surface

Considering a point P_{ij} on axis i and belonging to link that joins axis j with axis i. The axes of cylinder and links are expressed using dual vectors as L_c and L_{ij},

$$\begin{aligned} \mathsf{L}_c &= \mathbf{s}_c + \varepsilon(\mathbf{P}_{c_1} \times \mathbf{s}_c) \\ \mathsf{L}_{ij} &= \mathbf{s}_{ij} + \varepsilon(\mathbf{P}_{ij} \times \mathbf{s}_{ij}), \quad ij \in \mathcal{L}, \end{aligned} \tag{9}$$

where $\mathbf{s}_c$ and $\mathbf{s}_{ij}$ are the direction vectors for the cylinder axis and for the link respectively, and can be found using Equation (10),

$$\begin{aligned} \mathbf{s}_c &= \frac{\mathbf{P}_{c_2} - \mathbf{P}_{c_1}}{||\mathbf{P}_{c_2} - \mathbf{P}_{c_1}||} \\ \mathbf{s}_{ij} &= \frac{\mathbf{P}_{ji} - \mathbf{P}_{ij}}{||\mathbf{P}_{ji} - \mathbf{P}_{ij}||} \end{aligned} \tag{10}$$

The expression for the minimum distance between L_c and L_{ij} along the common normal line, a_{ij}, can be found from the dual dot product of the lines L_c and L_{ij} as shown in Equation (12). For the notation see Figure 4. In order to keep the links out of the restricted region, the constraints $a_{ij} \geq (R_C + R_{ij})$ are enforced in the optimization problem. In order to keep this obstacle avoidance constraint within the length of the cylinder, a condition is added to penalize this constraint when a link of the mechanism falls beyond the length of the cylinder. In Figure 4, point N_C lies on the axis of the cylinder. If it lies between P_{C1} and P_{C2}, then the constraint will be imposed, else the constraint will be penalized to be zero.

$$\mathbf{P}_{C1} + t_0 \mathbf{s}_c \leq \mathbf{N}_C \leq \mathbf{P}_{C1} + t_L \mathbf{s}_c \tag{11}$$

$$\mathsf{L}_c . \mathsf{L}_{ij} = \cos(\beta_{ij}) - \varepsilon a_{ij} \sin(\beta_{ij}), \quad i = 1 \ldots, n. \tag{12}$$

Where t_0 and t_L are the scalars defining the limits of the cylinder and $\mathbf{s}_c$ is the unit vector along the cylinder and defined in Equation (10).

Sphere constraint equations

Let S_C be the center of the sphere and R_S be its radius. When the region of interest is defined as a sphere, the region avoidance condition is created by imposing the distance to the center of the sphere to be greater than the sum of both radii, which yields again $2n$ quadratic inequality constraints for each configuration of the mechanism. The anchor points will be outside of the sphere if

$$(\mathbf{P}_{ij} - \mathbf{S}_C) . (\mathbf{P}_{ij} - \mathbf{S}_C) \geq (R_S + R_{ij})^2. \tag{13}$$

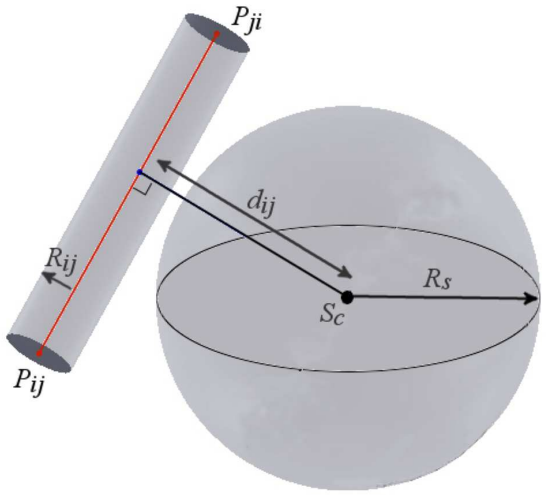

Fig. 5. Constraint Region Represented by a Spherical Surface

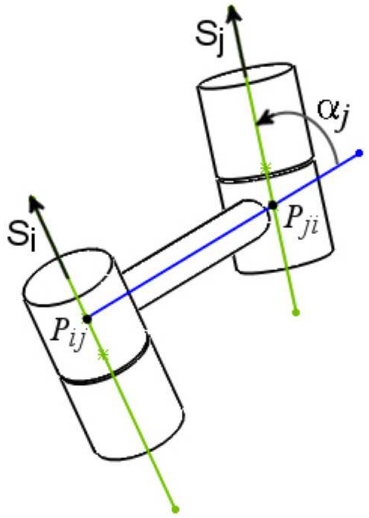

Fig. 6. Schematic diagram for the transmission angle

For straight links, to keep the whole link outside of the spherical region, calculate the perpendicular line from the sphere center to the line joining P_{ij} and P_{ji}, using Equation (14). The constraint $d_{ij} \geq (R_s + R_{ij})$ is used.

$$d_{ij} = \frac{\left|\left|(\mathbf{S}_c - \mathbf{P}_{ij}) \times (\mathbf{S}_c - \mathbf{P}_{ji})\right|\right|}{\left|\left|\mathbf{P}_{ji} - \mathbf{P}_{ij}\right|\right|}, \quad ij \in \mathcal{L}. \qquad (14)$$

2.2.3 Force transmission specifications

The concept of transmission angle, a common performance parameter for planar mechanisms, can be adopted for spatial linkages. The components of the forces as projected from link to axis are associated with friction, chatter and jamming at the joints, while the link-to-link projection is analogous to the traditional transmission angle; transmission indices have been defined by calculating the screw geometry of input and output joint axes [22], and it is independent on the realization of the links along the joints. However, problems associated with friction at the joints can be minimized by finding proper placement of the links with respect to the joint axes. This is the issue covered in the current optimization technique.

Let us consider α as the minimum acceptable transmission angle for force along the axis S_j versus force perpendicular to the axis, see Figure (6). Then we can state the constraints for each link of the mechanism as

$$\begin{aligned} &\frac{\mathbf{P}_{ji} - \mathbf{P}_{ij}}{\left|\left|\mathbf{P}_{ji} - \mathbf{P}_{ij}\right|\right|} \cdot \mathbf{s}_j = \cos(\alpha_j), \\ &|\cos(\alpha_j)| \leq \cos(\alpha) \end{aligned} \qquad (15)$$

Notice that the acceptable angle for revolute and prismatic joints needs to be different. Compared to revolute joints, prismatic joints are much more problematic in their application, they are sensitive to the direction and manner of load application. As shown in [37], if the friction force exceeds the component of the applied force along the slide direction the joint will jam. Considering such situations and assuming that the final value selected will be a function of the materials and lubrication, a generic value $\alpha = 60^o$ is chosen for revolute joints and $\alpha = 20^o$ for prismatic joints, while for cylindrical joints we use a compromise value and consider that the acceptable angle must be around $\alpha = 45^o$.

2.2.4 Planarity

For some cases, we may need spatial mechanisms to show a certain degree of planarity, at least in a given configuration, for instance at the reference configuration. This could yield quasi-foldable linkages, and it is also interesting for robotic hands used in human environments, where the fingers may be required to maintain planar shape at a reference configuration, similar to the extended human hand.

To ensure the planarity of the mechanism, Equation (16) can be applied for each joint of the mechanism to be at a distance less or equal to a certain value d from the desired reference plane. Consider the distance from a point, P, to a plane, as the smallest distance calculated from the point to any of the points on the plane, which happens along the perpendicular line. This can be defined as,

$$d = \frac{||Ax_0 + By_0 + Cz_0 + D)||}{\sqrt{(A^2 + B^2 + C^2)}} \qquad (16)$$

where the mechanism point is $P_{ij} = (x_0, y_0, z_0)$ and the desired reference plane is $Ax + By + Cz + D = 0$.

2.3 Configuration-dependent constraints

Some of the constraints on the performance of the mechanism, such as the obstacle avoidance, are a function of the configuration of the mechanism along a desired trajectory or for its whole workspace. In these cases, the constraints need to be enforced at a set of sampling points along the trajectory or workspace of the linkage. This is not too computationally costly for 1-dof mechanisms or when the motion of interest is a single trajectory, however it becomes more costly as the degrees of freedom of the mechanism increase, in which case a better strategy may be to consider the boundaries of the workspace instead. For the purpose of this article, the focus is on low-dof linkages or single one-dimensional trajectories, and the sampled trajectory strategy is used, for which a set of t equally-spaced points along the trajectory is considered.

In order to obtain the sampled trajectory, several strategies can be used. If the kinematics of the mechanism is fully defined, the trajectory can be generated using inverse or forward kinematics techniques. For those cases in which this approach is not available, a pre-defined trajectory may be given or interpolated ([38], [39]) and then the real trajectory can be approximated [40]. For other path planning techniques, see for instance [41].

For the CRR-RRR example, Figure 7 shows the required trajectory. For the Bennett mechanism, the kinematics is well known and an exact trajectory can be generated, shown in Figure 8.

Fig. 7. Desired trajectory of the CRR-RRR linkage

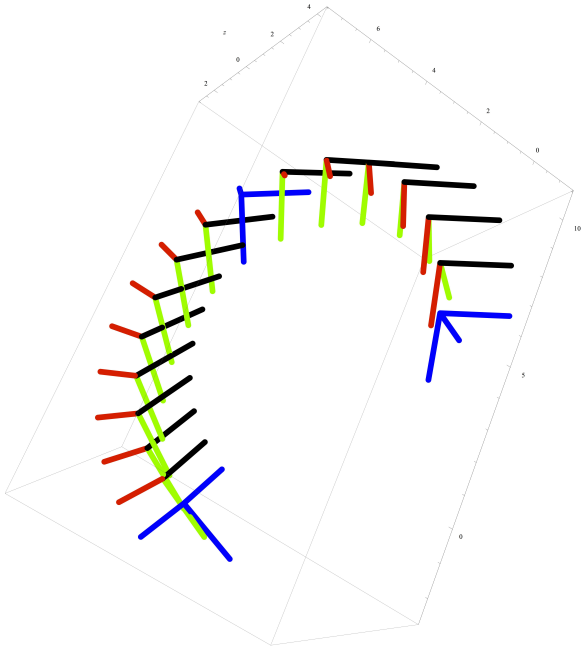

Fig. 8. Trajectory for the Bennett linkage

As an example, for the spherical region avoidance constraints on the anchor points, the total number of these inequality constraints increases to $2tl$, where t is the number of positions along the trajectory and l is the number of links in the mechanism,

$$(\mathbf{P}_{ij}^k - \mathbf{S}_C).(\mathbf{P}_{ij}^k - \mathbf{S}_C) \geq (R_S + R_{ij})^2, \quad k = 1, \ldots t, \quad ij \in \mathcal{L}. \qquad (17)$$

Every other constraint that depends on the configuration of the mechanism must be stated similarly.

3 Overall optimization strategy

Considering all the constraints and the objective function, the optimization problem involves the decision variables with their lower and upper limits, nonlinear objective functions, linear inequality constraints and nonlinear constraints. The nonlinearity in the objective function and constraints provide the main difficulty in solving the problem. A set of randomly generated solutions over those variable bounds indicate that only few solutions are feasible. Such a severe geometry of the feasible region makes the problem even more difficult to solve. For this reason the hybrid genetic optimization algorithm was found suitable to reach at a global minimum point.

For each spatial mechanism, the optimization problem is developed as shown in Equation (18). Due to the co-

existence of linear and nonlinear constraints in the optimization problem, the linear constraints are mostly satisfied easily, however the nonlinear constraints may not be satisfied as easily. Thus, depending on the problems and the solution obtained, the Augmented Lagrangian Genetic Algorithm (ALGA) [42] is used with a penalty parameter to find the feasible region. In ALGA, a subproblem is formulated by combining the objective function and nonlinear constraint function using the Lagrangian and the penalty parameters, see Equation (19). A sequence of such optimization problems are approximately minimized using the genetic algorithm such that the linear constraints and bounds are satisfied.

$$\begin{aligned} &\min f(x), such\ that \\ &\qquad g_i(x) \le 0, \quad i = 1,\dots k \\ &\qquad g_{eq_i}(x) = 0, \quad i = k+1,\dots kt \\ &\qquad Ax \le b \\ &\qquad A_{eq}x = b_{eq} \\ &\qquad lb \le x \le lu \end{aligned} \tag{18}$$

$$\begin{aligned} F(x,\lambda,s,\rho) = f(x) - \sum_{i=1}^{k} \lambda_i s_i log(s_i - g_i(x)) + \sum_{i=k+1}^{kt} \lambda_i g_{eq_i}(x) \\ + \frac{\rho}{2} \sum_{i=k+1}^{kt} g_{eq_i}(x)^2 \end{aligned} \tag{19}$$

In Equations (18) and (19), g(x) represents the nonlinear inequality constraints, $g_{eq}(x)$ the nonlinear equality constraints, k the number of nonlinear inequality constraints, and kt the total number of nonlinear constraints. A is an $m \times n$ matrix, x is an $n \times 1$ column vector of variables, and b is an $m \times 1$column vector of constants.

The parameters λ_i are Lagrange multiplier estimates, s_i are nonnegative shifts and ρ is the positive penalty parameter. *Mathematica*® is used to formulate the equations and to create *Matlab*® executable files. Depending on the nature and complexity of the problem, the GA in *Matlab*® took from seconds to considerable amount of time to converge to optimum solution. For the illustration of the algorithm, two examples are presented. These examples are selected to cover closed linkages with different applications and design requirements.

4 Examples

The above procedure has been applied to a spatial, closed-loop CRR-RRR, and to a Bennett mechanism. The *Mathematica*® code for these examples can be downloaded from the project webpage, http://robotics.engr.isu.edu/. The parameters used to run the genetic algorithm are the chromosome length, that is, the number of variables in the problem; the initial population; and the initial value for the penalty parameters. From multiple trials, we found a probability crossover of 0.8 was good so that majority of the population is regenerated after each generation cycle while keeping the best solutions found. A stopping criterion is set so that the algorithm stops when the population has fully converged.

4.1 CRR-RRR mechanism

The spatial, closed-loop CRR-RRR mechanism has one degree of freedom and with the end effector located at the intersection of the serial CRR and the serial RRR chains as shown in Figure 3(a). The mechanism has been designed to be used as an exoskeleton device for thumb motion [43]. Additional constraints are added to control the position and size of the mechanism, and to reduce physical interference with the user.

The kinematic synthesis of the mechanism alone yields 147 nonlinear equations in 97 variables, which makes it challenging to add more constraints in the synthesis process. The output of the synthesis ensures the trajectory of the end effector but does not provide any insight regarding size and placement of the linkage. The use of the link-based optimization as a second stage is used to adapt the linkage to those performance parameters, and illustrates the dramatic changes in the linkage that can be obtained with this method, while still targeting the same trajectory.

4.1.1 Problem Definition and Formulation

Consider one of the solutions obtained through the synthesis of the CRR-RRR linkage as seen in Figure 9. The screw axis in Plücker coordinates are given in the Table 1. The black lines are the links of the mechanism, drawn by connecting the common normal points of consecutive axes. The green-colored lines represent the joint axes. The cylinder represents the user's hand and forearm, with which the mechanism should not interfere. As we can see in this initial solution, some of the joints interfere with the volume of the cylinder, and the link sizes are also not controlled, ranging from very small to very large. This initial solution is not acceptable in terms of compactness, manufacturability and assembly point of view. Therefore, a post-optimization of the design was found necessary.

In order to see the effect of each optimization step, the optimization of length, region avoidance and force transmission have been tested one by one and finally all at a time. In all cases, the range of the required link lengths have been set between 20mm and 150mm. The cylinder position and size are shown in Table 2. The optimization problem was implemented in *Matlab*® code, and for this particular example, the algorithm converges to a solution in approximately 45 generations.

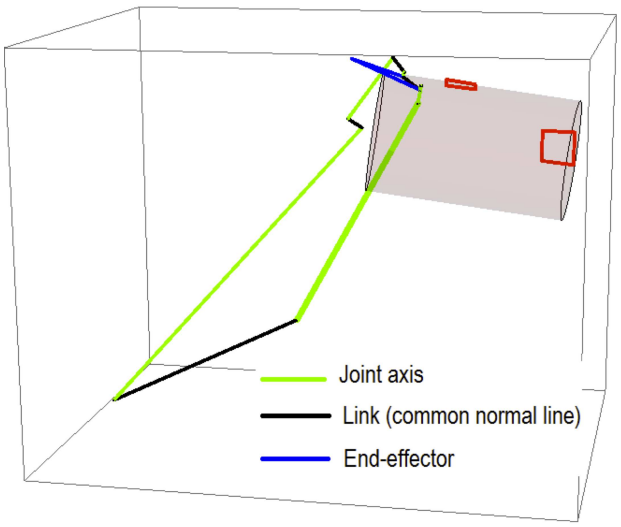

Fig. 9. Initial CRR-RRR Mechanism. Black links are located at the common normal lines between joints.

Table 1. Plucker Coordinates of the CRR-RRR Screw axes [*mm*]

Axis	$s_i + \varepsilon(s_i^0)$
1	$\begin{Bmatrix} -0.397 \\ 0.675 \\ -0.622 \end{Bmatrix} + \varepsilon \begin{Bmatrix} -295.833 \\ -191.017 \\ -18.657 \end{Bmatrix}$
2	$\begin{Bmatrix} -0.224 \\ 0.480 \\ -0.848 \end{Bmatrix} + \varepsilon \begin{Bmatrix} -108.798 \\ -49.319 \\ 0.889 \end{Bmatrix}$
3	$\begin{Bmatrix} 0.253 \\ -0.523 \\ 0.814 \end{Bmatrix} + \varepsilon \begin{Bmatrix} 147.218 \\ 73.695 \\ 1.551 \end{Bmatrix}$
4	$\begin{Bmatrix} 0.482 \\ -0.109 \\ 0.870 \end{Bmatrix} + \varepsilon \begin{Bmatrix} -139.844 \\ 246.543 \\ 108.428 \end{Bmatrix}$
5	$\begin{Bmatrix} 0.591 \\ -0.002 \\ 0.806 \end{Bmatrix} + \varepsilon \begin{Bmatrix} -179.429 \\ 349.744 \\ 132.504 \end{Bmatrix}$
6	$\begin{Bmatrix} -0.642 \\ 0.317 \\ -0.698 \end{Bmatrix} + \varepsilon \begin{Bmatrix} -48.561 \\ -369.995 \\ -123.356 \end{Bmatrix}$

When minimizing only the total link size, we obtain the link lengths shown in Table 3. However most of the mechanism joints lie inside the restricted region, as we can see in

Table 2. Cylinder position and size in [*mm*]

P_{c1}	P_{c2}	R_C
$\begin{Bmatrix} 274.62 \\ -213.50 \\ 605.01 \end{Bmatrix}$	$\begin{Bmatrix} 71.06 \\ -239.32 \\ 634.43 \end{Bmatrix}$	63.26

Figure 10.

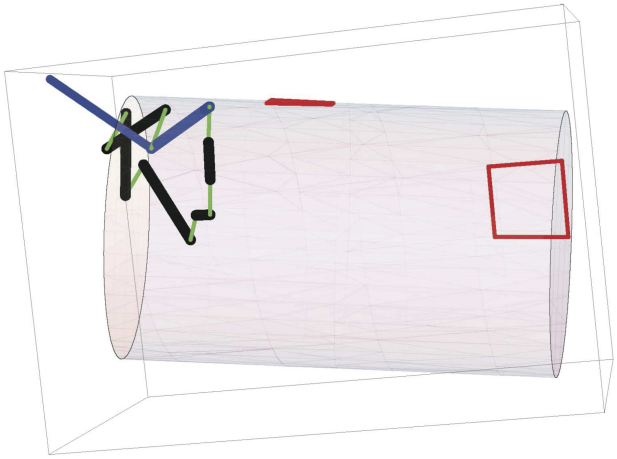

Fig. 10. Mechanism obtained after link length constraints used

Considering the region-avoidance problem alone, the solution shows that all the links at the different task positions along the trajectory of the linkage stay out of the the restricted region, see Figure 11 . However, most of the link sizes are very large, see Table 3.

Considering the link optimization, obstacle avoidance and the force transmission simultaneously gives a better result in terms of fulfilling the requirements. See Figure 12 for the final solution and Figure 13 for a sampling of the motion to avoid the obstacle. The link lengths are shown in Table 3. Figure 14 shows the CAD implementation of the optimized solution.

The objective function (F) obtained for link-size optimization is 2.0785×10^4, for region avoidance 1.2306×10^5, and for link size and region avoidance is 6.6886×10^4.

4.2 The Bennett mechanism

The Bennett Linkage is a 4R spatial closed chain. Bennett discovered the geometric relations that ensure that this chain can move with one degree of freedom. Research on the Bennett linkage has focused on its instantaneous kinematic geometry and its finite-position synthesis. In this study, the Bennett mechanism is used as a hinge for a cabinet door, Figure 15. The kinematic synthesis is performed to obtain

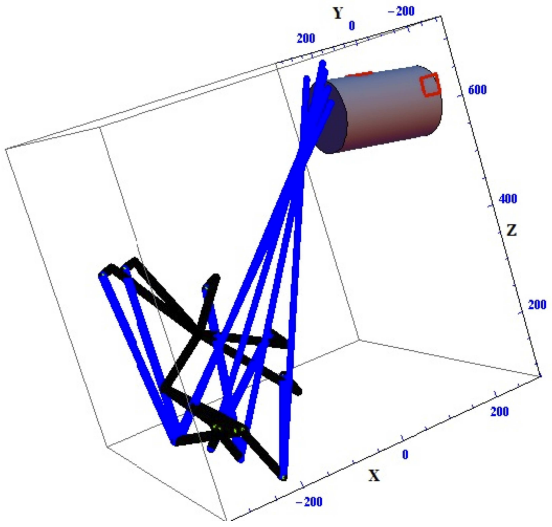

Fig. 11. Different configurations of the mechanism obtained after region avoidance constraint is used

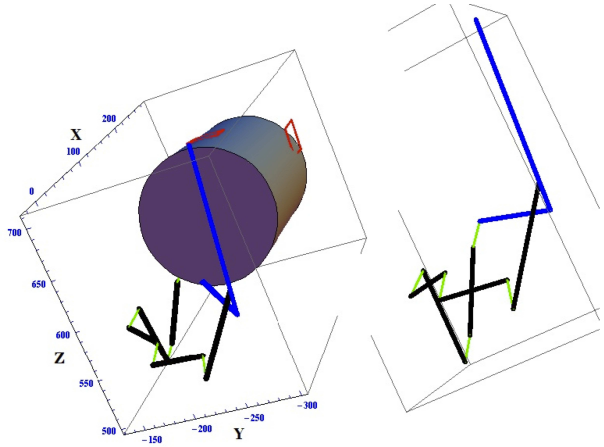

Fig. 12. Mechanism obtained after optimizing region avoidance, overall length and force transmission

the desired trajectory. To get the optimum solution considering manufacturability, obstacle avoidance and smoothness of motion, the link-based optimization technique outlined above is implemented.

4.2.1 Problem Definition and Formulation

The initial implementation from the synthesis stage uses the screw axes in Plücker coordinates as shown in Table 4. In this particular example the mechanism created by connecting the common normal lines is fairly compact (Figure 16); however, some of the dimensions are too small from a manufacturing and assembly point of view; for instance, the smallest length is 5mm and the offset for the joints along the axes is almost zero. In addition to this, part of the mechanism

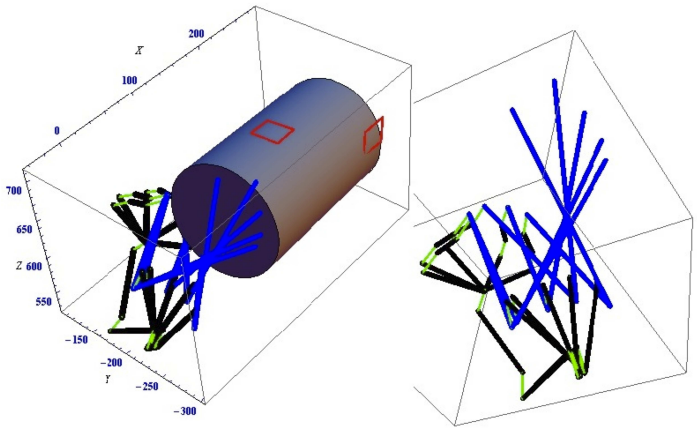

Fig. 13. Motion of the mechanism obtained after optimizing region avoidance, overall length and force transmission. Five positions along the trajectory are reached by the mechanism while avoiding the obstacle. (Green for the joint axis, black for linkage of the mechanism and blue for the end-effector)

Table 3. Link Lengths [mm] obtained through different optimization stages: (1) Common normal lines directly from synthesis; (2) Link-size optimization;(3) Region avoidance; (4) Link size and region avoidance

Result from	L_{12}	L_{23}	L_{34}	L_{45}	L_{56}	L_{61}	L_{4Ef}
(1)	0.31	0.50	25.36	31.44	18.36	26.90	55.87
(2)	20.00	57.13	76.50	46.96	40.04	51.18	20.00
(3)	244.91	46.43	543.16	125.93	184.05	277.83	671.00
(4)	150.49	57.13	138.75	46.96	109.92	150.66	151.00

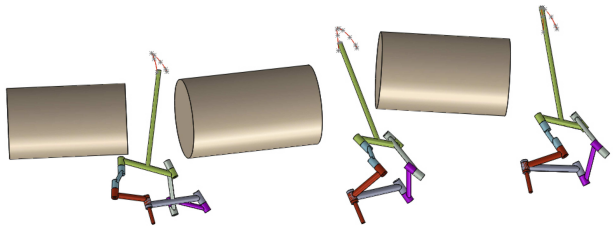

Fig. 14. The CAD model for the final optimized solution at three different configurations

lies inside the cabinet, that is, inside of the restricted region. Considering minimum and maximum lengths, and obstacle avoidance constraints, the solution may be a less compact but applicable mechanism.

Figure 17 shows the optimized Bennett mechanism with imposed constraints of minimum link length of 30mm, max-

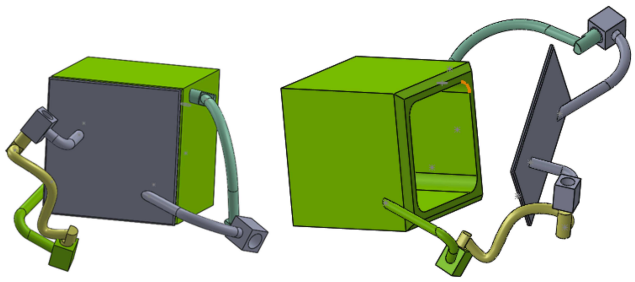

Fig. 15. The Bennett Linkage used as a hinge and a cabinet door (Courtesy of PsiStar Solutions)

Table 4. Plucker Coordinates of the Bennett Linkage Screw Axes [mm]

Axis	$s_i + \varepsilon(s_i^0)$
1	$\begin{Bmatrix} 0.301 \\ 0.827 \\ 0.475 \end{Bmatrix} + \varepsilon \begin{Bmatrix} -5.12 \\ 1.901 \\ -0.068 \end{Bmatrix}$
2	$\begin{Bmatrix} 0.588 \\ 0.809 \\ 0.009 \end{Bmatrix} + \varepsilon \begin{Bmatrix} -2.970 \\ 2.210 \\ -4.896 \end{Bmatrix}$
3	$\begin{Bmatrix} 0.798 \\ -0.372 \\ 0.475 \end{Bmatrix} + \varepsilon \begin{Bmatrix} -1.901 \\ -4.164 \\ -0.068 \end{Bmatrix}$
4	$\begin{Bmatrix} 0.988 \\ -0.156 \\ 0.009 \end{Bmatrix} + \varepsilon \begin{Bmatrix} -0.381 \\ -2.675 \\ -4.896 \end{Bmatrix}$

imum link length of 60mm and an offset length of 15mm. As we can see, the joints have now enough offset for assembly, and the link lengths also fall within the range of the specified constraints. However, part of the mechanism is still inside of the restricted region, which is the cabinet; therefore, additional constraints to avoid this problem are required.

Obstacle avoidance

The cabinet has the shape of a cube. To simplify the problem, an inscribed sphere is considered to define the region avoidance constraint. An increment δ for tha radius is used to take into consideration the thickness of the links, to yield a sphere radius $S_R + \delta$. The obstacle avoidance constraint keeps the mechanism on one side of the door and out of the cube, Figure 18. However, the link sizes are much longer than the perceived optimal solution. Finally, by incorporating all the constraints including link length, offset

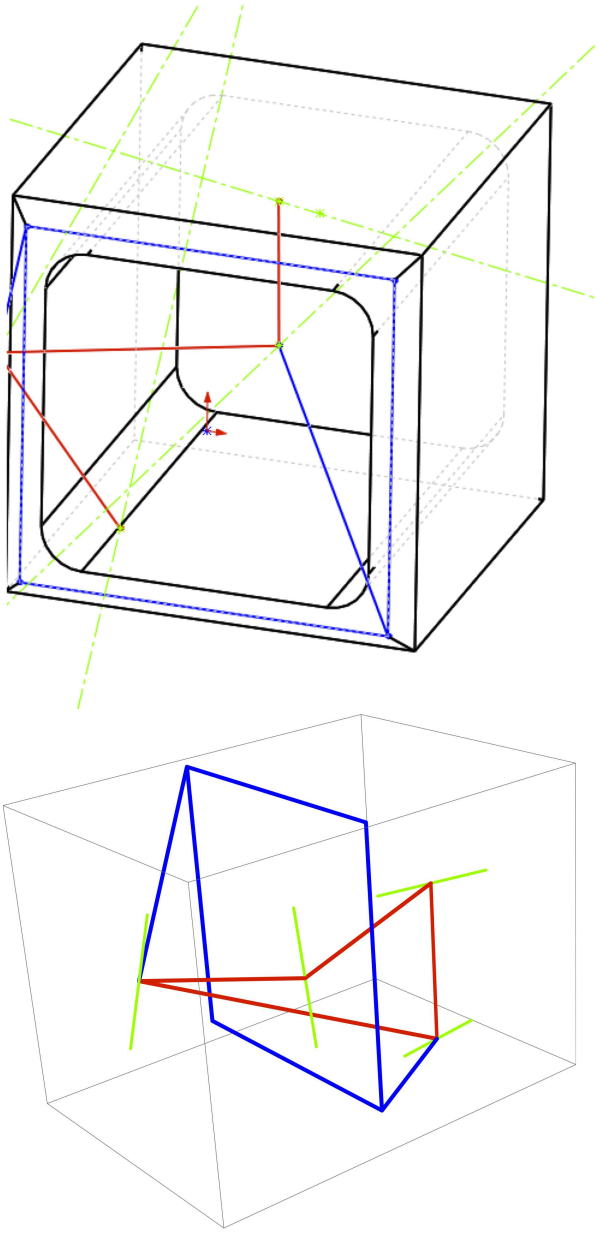

Fig. 16. Initial solution of the Bennett linkage

length and obstacle avoidance, a better solution is found and shown in Figure 19. The motion of the linkage can be seen in Figure 20.

5 CONCLUSIONS

In the design of spatial linkages for a desired motion, a great deal of flexibility is allowed in the choice of the link location and dimensions. The optimization presented in this paper is used to modify the links of the linkage in order to fulfill additional performance requirements, such as total length, force transmission, obstacle avoidance or geometry

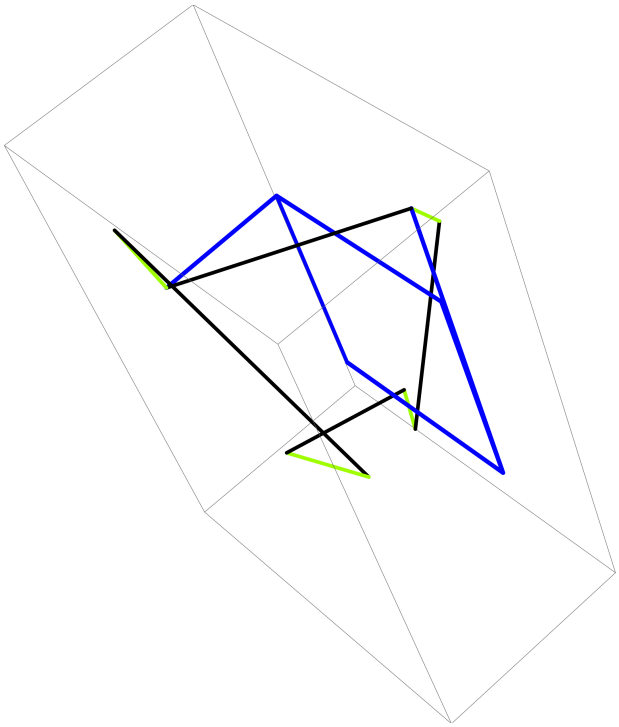

Fig. 17. Optimized Bennett linkage with only link length constraints

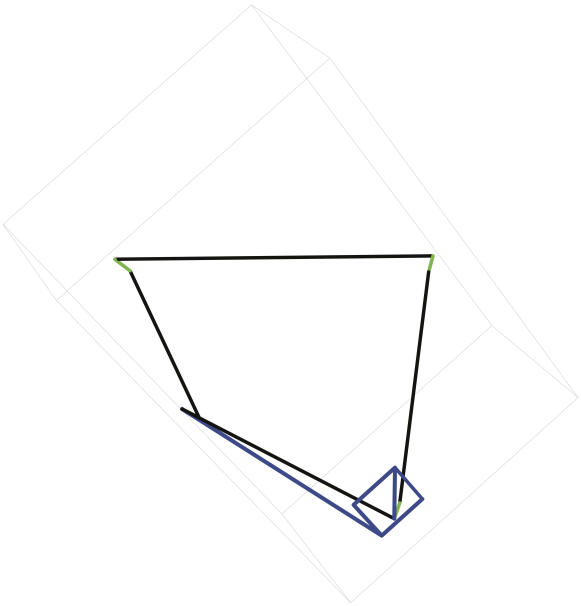

Fig. 18. Mechanism with only obstacle avoidance and offset constraint. The blue square corresponds to the cabinet door.

at a given configuration. It is our experience that trying to fulfill these requirements with a manual manipulation of the links is tedious and overall difficult.

The method has been implemented using a hybrid genetic algorithm plus gradient-based local optimization approach in *Matlab*®. This approach yields better results than the single genetic algorithm approach as the number or nonlinear constraints increases.

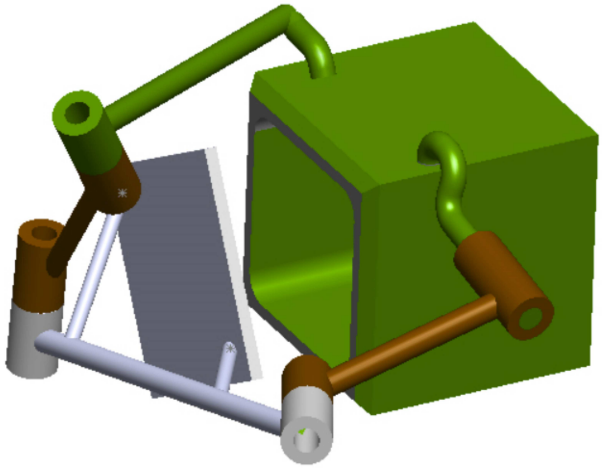

Fig. 19. Mechanism obtained with link length, offset length and obstacle avoidance constraints.

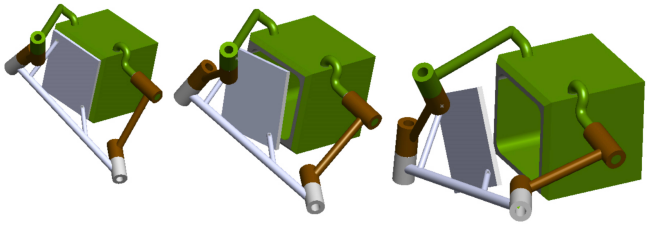

Fig. 20. Motion of the final design for the cabinet linkage

The methodology is general enough that any link-based requirement can be added to the optimization, either within the objective function or as additional constraints. It is straightforward to define the links in a CAD environment as anchored in points sliding along the joint axes of the linkage, making the application of the optimization results automatic. The algorithm is also flexible so that it can be applied to the overall mechanism or just to a part of it.

The results obtained show that dramatic changes in the final design of the mechanism can be obtained by using this method, making it a useful tool for the designer of spatial mechanisms with arbitrarily-located axes. The links are here defined as straight lines between anchored points at the joints; in a future extension, the links will be allowed to have a curved shape in order to increase the solution space.

Acknowledgements

This work is supported by the National Science Foundation under Grant No. 1208385. The content is solely the author's responsibility.

References

[1] Garcia de Jalon, J., and Bayo, E., 1994. *Kinematic and Dynamic Simulation of Multibody Systems*. Springer-Verlag.

[2] Minaar, R., Tortorelli, D., and Snyman, J., 2001. "On nonassembly in the optimal dimensional synthesis of planar mechanisms". *Structural Multidisciplinary Optimization,* ***21***, pp. 345–354.

[3] Jensen, J., and Hansen, O., 2006. "Dimensional synthesis of spatial mechanisms and the problem of non-assembly". *Multibody System Dynamics,* ***15***, pp. 107–133.

[4] Hansen, O., 2002. "Synthesis of mechanisms using time-varying dimensions". *Multibody System Dynamics,* ***7***, pp. 127–144.

[5] Hobson, M., and Torfason, L., 1975. "Computer optimization of polycentric prosthetic knee mechanisms". *Bulletin of Prosthetic Research,* ***10***, pp. 187–201.

[6] Jin, D., Zhang, R., Dimo, H., Wang, R., and Zhang, J., 2003. "Kinematic and dynamic performance of prosthetic knee joint using six-bar mechanism". *Rehabilitation Research and Development,,* ***40***, pp. 39–48.

[7] Nokleby, S., and Podhorodeski, R., 2006. "Optimization-based synthesis of Grashof geared five-bar mechanisms". *ASME Journal of Mechanical Design,* ***138***, pp. 529–534.

[8] Kinzel, E., Schmiedeler, J., and Pennock, G., 2006. "Kinematic synthesis for finitely separated positions using geometric constraint programming". *Mechanism and Machine Theory,* ***128***, pp. 1070–1079.

[9] Cabrera, J., Simon, A., and Prado, M., 2002. "Optimal synthesis of mechanisms with genetic algorithms". *Mechanism and Machine Theory,* ***37***, p. 11651175.

[10] Acharyya, S., and Mandal, M., 2009. "Performance of eas for four-bar linkage synthesis". *Mechanism and Machine Theory,* ***44***, pp. 1784–1794.

[11] Shieh, W.-B., Tsai, L., and Azarm, S., 1997. "Design and optimization of a one-degree-of-freedom six-bar leg mechanism for a walking machine". *Journal of Robotic Systems,* ***14(12)***, pp. 871–880.

[12] Yao, J., and Angeles, J., 2000. "Computation of all optimum dyads in the approximate synthesis of planar linkages for rigid-body guidance". *Mechanism and Machine Theory,* ***35***, pp. 1065–1078.

[13] Zhou, H., 2009. "Dimensional synthesis of adjustable path generation linkages using the optimal slider adjustment". *Mechanism and Machine Theory,* ***44***(10), pp. 1866–1876.

[14] Shen, Q., Al-Smadi, Y., Martin, P., Russell, K., and Sodhi, R., 2009. "An extension of mechanism design optimization for motion generation". *Mechanism and Machine Theory,* ***44***, pp. 1759–1767.

[15] Stock, M., and Miller, K., 2003. "Optimal kinematic design of spatial parallel manipulators: Application to linear delta robot". *ASME Journal of Mechanical Design,* ***125***, pp. 292–301.

[16] Arsenault, M., Boudreau, and Roger, 2004. "The synthesis of three-degree-of-freedom planar parallel mechanisms with revolute joints (3-RRR) for an optimal singularity-free workspace". *Journal of Robotic Systems,* ***21***(5), pp. 259–274.

[17] Altuzarra, O., Hernandez, A., Salgado, O., and Angeles, J., 2009. "Multiobjective optimum design of a symmetric parallel schnflies-motion generator". *ASME Journal of Mechanical Design,* ***131***, pp. 0310021–03100211.

[18] Kim, H.S., a. T., 2003. "Design optimization of a cartesian parallel manipulator". *ASME Journal of Mechanical Design,* ***125***, pp. 43–51.

[19] Merlet, J., 2006. "Jacobian, manipulability, condition number, and accuracy of parallel robots". *ASME Journal of Mechanical Design,* ***128***, pp. 199–206.

[20] Khan, W., and Angeles, J., 2006. "The kinetostatic optimization of robotic manipulators: The inverse and the direct problems". *ASME Journal of Mechanical Design,* ***128***, pp. 168–178.

[21] Altuzarra, O., Pinto, C., Sandru, B., and Hernandez, A., 2011. "Optimal dimensioning for parallel manipulators: Workspace, dexterity, and energy". *ASME Journal of Mechanical Design,* ***133***, pp. 0410071–0410077.

[22] Chen, C., and Angeles, J., 2006. "Generalized transmission index and transmission quality for spatial linkages". *Mechanism and Machine Theory,* ***42***, pp. 1225–1237.

[23] Wu, C., Liu, X.-J., Wang, L., and Wang, J., 2010. "Optimal design of spherical 5r parallel manipulators considering the motion/force transmissibility". *ASME Journal of Mechanical Design,* ***132***, pp. 0310021–03100210.

[24] Ravani, B., and Roth, B., 1983. "Motion synthesis using kinematic mappings". *ASME Journal of Mechanism, Transmissions, and Automation in Design,* ***105***, pp. 460–467.

[25] Hong, B., and Erdman, A., 2005. "A method for adjustable planar and spherical four-bar linkage synthesis". *ASME Journal of Mechanical Design,* ***127 (3)***, pp. 456–463.

[26] Hayes, M., Luu, T., and Chang, X.-W., 2004. "Kinematic mapping application to approximate type and dimension synthesis of planar mechanisms". In Advances in Robot Kinematics, J. Lenarcic and C. Galletti, eds., Kluwer Academic Publishers, pp. 41–48.

[27] Anoop, M., and Samson, A., 2009. "Optimal synthesis of spatial mechanism using genetic algorithm". In 10th National Conference on Technological Trends (NCTT09), pp. 26–32.

[28] Kosinska, A., Galicki, M., and Kedzior, K., 2003. "Design and optimization of parameters of delta-4 parallel

manipulator for a given workspace". *Journal of Robotic Systems,* ***20(9)***, pp. 539–548.

[29] Lum, M., Rosen, J., Sinanan, M., and B, H., 2004. "Kinematic optimization of a spherical mechanism for a minimally invasive surgical robot". In Robotics and Automation, 2004. Proceedings. ICRA '04. 2004 IEEE International Conference on, Vol. 1, pp. 829–834 Vol.1.

[30] Nielsen, J., and Roth, B., 1998. "Formulation and solution for the direct and inverse kinematics problems for mechanisms and mechatronics systems". In *Computational Methods in Mechanical Systems*. Springer, pp. 33–52.

[31] Niku, S. B., 2001. *Introduction to robotics: analysis, systems, applications*, Vol. 7. Prentice Hall New Jersey.

[32] Craig, J. J., 1989. *Introduction to robotics*, Vol. 7. Addison-Wesley Reading, MA.

[33] Fischer, I., 1998. *Dual-number methods in kinematics, statics and dynamics*. CRC Press.

[34] Ketchel, J. S., and Larochelle, P. M., 2008. "Self-collision detection in spatial closed chains". *Journal of Mechanical Design,* ***130***(9), p. 092305.

[35] Xiao, J., Xu, J., Shao, Z., Jiang, C., and Pan, L., 2007. "A genetic algorithm for solving multi-constrained function optimization problems based on ks function". In Evolutionary Computation, 2007. CEC 2007. IEEE Congress on, pp. 4497–4501.

[36] Hayward, V., Choksi, J., Lanvin, G., and Ramstein, C., 1994. "Design and multi-objective optimization of a linkage for a haptic interface". In *Advances in Robot Kinematics and Computational Geometry*. Springer, pp. 359–368.

[37] Waldron, K. J., and Kinzel, G. L., 2004. *Kinematics, Dynamics, and Design of Machinery*, 2nd edition ed. Wiley.

[38] Gfrerrer, A., 2000. "Study's kinematic mapping - a tool for motion design". *Recent Advances in Robot Kinematics*, pp. 7–16.

[39] Klawitter, D., 2010. *Toolbox-Kinematics*. http://www.mathworks.com/matlabcentral/fileexchange/27114-toolbox-kinematics.

[40] Perez, A., and McCarthy, J. M., 2000. "Dimensional synthesis of spatial rr robots". In *Advances in Robot Kinematics*. Springer, pp. 93–102.

[41] Su, H.-J., Dietmaier, P., and McCarthy, J. M., 2003. "Trajectory planning for constrained parallel manipulators". *Journal of mechanical design,* ***125***(4), pp. 709–716.

[42] Conn, A., Gould, N., Toint, and Philippe, 1991. "A globally convergent augmented lagrangian algorithm for optimization with general constraints and simple bounds". *SIAM Journal on Numerical Analysis,* ***28***(2), pp. 545–572.

[43] Yihun, Y., Miklos, R., Perez-Gracia, A., Reinkensmeyer, D. J., Denney, K., and Wolbrecht, E. T., 2012. "Single degree-of-freedom exoskeleton mechanism design for thumb rehabilitation". In Engineering in Medicine and Biology Society (EMBC), 2012 Annual International Conference of the IEEE, IEEE, pp. 1916–1920.